iim$$$6147

International Immunology, Vol. 9, No. 1, pp. 43–51

Molecular characterization of the diabetes-associated mouse MHC class II protein, I-A^{g7}

Boris Reizis, Miriam Eisenstein[1], Jana Bočková, Stephanie Könen-Waisman, Felix Mor, Dana Elias and **Irun R. Cohen**

Department of Immunology and [1]Chemical Services, The Weizmann Institute of Science, Rehovot 76100, Israel

Keywords: autoimmunity, non-obese diabetic mice, peptides

Abstract

The MHC class II molecule of the non-obese diabetic (NOD) mice, I-A^{g7}, is associated with susceptibility to autoimmune diabetes. To try to understand the molecular basis of this association, we analyzed the peptide binding properties and intracellular behavior of I-A^{g7} in comparison with other I-A haplotypes. We found that I-A^{g7} molecules manifested normal intracellular trafficking and lifespan, and a small but clearly detectable fraction of I-A^{g7} in the cells formed SDS-resistant compact dimers. The binding of an antigenic reference peptide to I-A^{g7} was stable and was accompanied by compact dimer formation. Our analysis of the binding specificity of I-A^{g7} revealed a peptide binding motif of nine amino acids with a degenerate position at P1 and three conserved anchor positions: P4, P6 and P9. An allele-specific preference for negatively charged residues was found at P9, apparently due to the presence of the rare Ser residue at position 57 of the I-A^{g7} β chain. These findings could have implications for the mechanisms of MHC-mediated susceptibility to autoimmune diabetes in the NOD mice.

Introduction

Mice of the non-obese diabetic (NOD) strain spontaneously develop autoimmune insulitis and diabetes resembling the human autoimmune disease insulin-dependent diabetes mellitus (1,2). Genetic analysis and studies with transgenic animals suggest an important role for MHC class II products in the disease (3). The only expressed MHC class II molecule in the NOD mouse is a unique I-A allele, I-A^{g7}, which appears essential for susceptibility to diabetes (3). The I-A^{g7} molecule is identical to another I-A allele, I-A^{d}, except for 17 amino acid substitutions in the first external domain of the β chain (4). In particular, I-A^{g7} features rare His–Ser residues, in place of the usual Pro–Asp residues, at positions 56–57 of the β chain. Interestingly, polymorphism at β57 in the MHC class II molecule of the human correlates with susceptibility to diabetes and pemphigus vulgaris (5). Thus, the association of I-A^{g7} with diabetes might have general implications for the associations of MHC class II products with autoimmune diseases (6).

The molecular basis of the association of I-A^{g7} with diabetes is unknown. In this regard, two unusual properties of I-A^{g7} were reported. First, Reich *et al*. (7) noticed the uncommon occurrence of negatively charged residues near the C-terminus of I-A^{g7}-bound peptides and correlated it with the rare β56His–β57Ser residues of I-A^{g7}. However, an overall peptide binding specificity of I-A^{g7} was not obvious; moreover, the binding specificities of other mouse I-A alleles are similarly obscure (8). Second, Carrasco-Marin *et al*. (9) observed that, relative to other MHC class II alleles, only a minor fraction of I-A^{g7} in the cell is occupied by stably bound peptides as judged by SDS stability analysis. These authors further suggested that the I-A^{g7} molecule is defective in peptide binding and may be unable to form stable complexes with peptides. However, two facts argue against this notion: natural peptide ligands can be isolated from I-A^{g7} (7), and both spontaneous and induced peptide-specific CD4^{+} T cell responses are routinely observed in NOD mice. Therefore, the distinct biochemical properties of I-A^{g7}, possibly contributing to the association of I-A^{g7} with diabetes, are poorly defined. To this end, we studied the peptide binding characteristics and the intracellular behavior of I-A^{g7} in comparison with other I-A alleles.

Methods

Animals

Inbred SJL/J (H-2^{s}), PL/J (H-2^{u}) and C3H/HeJ (H-2^{k}) were obtained from Jackson (Bar Harbor, ME); BALB/c (H-2^{d}) mice

Correspondence to: I. R. Cohen

Transmitting editor: L. Steinman

Received 20 May 1996, *accepted* 17 September 1996

were from Harlan Olac (Bicester, UK). The colony of NOD/Lt (H-2^{g7}) mice, originally provided by Dr E. Leiter (Jackson), was maintained at the animal breeding center of this institute. Two-month-old diabetes-free NOD mice were used for the study.

Peptides

Peptides were synthesized with an automated multiple peptide synthesizer (AMS 422; Abimed, Langenfeld, Germany) using standard Fmoc chemistry. The quality of each peptide was confirmed by analytical reverse-phase HPLC. The peptides were lyophilized and dissolved at 20 mg/ml in DMSO to ensure complete solubilization.

Substituted polyAla peptides

The peptide binding motifs of most MHC class II molecules appear to consist of a nine amino acid sequence with four major anchor positions: P1, P4, P6 and P9 (10). Our preliminary computer modeling suggested that I-A^{g7} might have a similar motif. Therefore, we designed a set of nonamer polyAla peptides substituted at positions 1, 4, 6 and 9. The substitutions were chosen to represent major classes of amino acid: aliphatic (Leu), aromatic (Tyr), small polar (Thr), large polar (Gln), negatively charged (Glu) and positively charged (Lys); other substitutions were introduced as indicated. Preliminary computer modeling of I-A^{g7} suggested that an Arg residue would not be accommodated at either P6 or P9, but is favorable at P7. Therefore, two Arg residues were introduced at positions 7 and 8, both to increase binding and to prevent possible binding frameshifts in either direction. The reference peptides were AAAAAARRE for P1 and P4, AAALAARRA for P9, and AAALAARRE for P6. Limited substitutions were also tested at positions 5 and 7 using a AAALAAAAE reference peptide.

Peptide binding assay

We measured peptide binding using a competitive inhibition assay of T cell line proliferation in response to a reference peptide presented by fixed antigen-presenting cells (11). This assay was used because it correlates well with a binding assay using purified class II molecules (11,12); in addition, the binding of peptides to purified I-A^{g7} proteins was reported to be difficult to measure (9). The reference peptide for binding to I-A^{g7} was peptide 166–185 (EEIAQVATISANGDKDIGNI) of the mouse HSP60 protein, designated p12, which is immunogenic in NOD mice (J. Bočková *et al.*, in preparation). The reference peptide for binding to I-A^{d} was peptide 458–74 (NEDQKIGIEIIKRTLKI) of the human HSP60 protein, also designated CP1h, which is immunogenic in BALB/c mice (13). The reference T cells were CD4^{+}, TCR$\alpha\beta^{+}$ long-term lines specific for peptides p12 and CP1h presented by I-A^{g7} and I-A^{d} respectively.

Activated peritoneal macrophages were isolated from mice that had been injected i.p. 3 days before with 0.1 mg concanavalin A. The cells were resuspended in DMEM with 10% FCS, seeded at 10^5/well into 96-well round-bottom plastic plates and incubated for 2 h at 37°C. The adherent macrophage monolayers were washed with PBS, fixed with 0.1% glutaraldehyde for 1 min, and washed with 1 M lysine/PBS and then with PBS. The peptides were added in citrate-phosphate buffer (25 mM citric acid, 50 mM Na_2HPO_4, 150 mM NaCl), pH 5.0 or 7.2, and incubated at 37°C for the indicated periods. For the competition assay, a single concentration of a stimulatory peptide (1 μM for p12 and 4 μM for CP1h) and a test peptide (either a single concentration of 400–1000 μM or a dose range) were added simultaneously. Peptides causing no inhibition of the response (Z1a TCRβ 70–81, SQGDFFLTLESA, and 104–115, GHGTKLSVLEDL, for I-A^{g7} and I-A^{d} respectively) were used as negative controls. The wells were washed with PBS, resting cells (5×10^4/well in DMEM with 10% FCS) of the peptide-specific T cell line were added and [^{3}H]thymidine incorporation was determined 3 days later. The results represent the mean c.p.m. ± SD of duplicate cultures.

Cell labeling and immunoprecipitation

For metabolic labeling, freshly isolated splenocytes were resuspended (2×10^7/ml) in methionine-free DMEM supplemented with 10% dialyzed FCS and incubated for 1 h at 37°C. The cells were pulsed for indicated periods of time with 100 μCi/ml [^{35}S]methionine and washed twice in cold PBS. For pulse–chase experiments, the pulsed cells were resuspended (10^7/ml) in complete DMEM with 10% FCS and incubated at 37°C for the indicated periods of time. For membrane labeling, viable splenocytes were isolated by centrifugation over a density gradient of 65% Percoll, washed in PBS and labeled on ice with ^{125}I by lactoperoxidase-catalyzed iodination.

Labeled cells were lysed using a buffer containing 1% NP-40, 50 mM Tris–HCl, pH 8.0, 150 mM NaCl, 1 mM EDTA, 1 mM phenylmethylsulfonyl fluoride and 10 μg/ml aprotinin. The lysates were centrifuged at 16000 *g* for 30 min, and precleared with Protein A–Sepharose and then with Protein A–Sepharose precoated with rabbit anti-mouse IgG serum. In some experiments, the protocol of Germain and Rinker (14) was used with minor modifications. Briefly, the precleared lysates were divided into aliquots and either left untreated or adjusted to pH 5.0 by the addition of acetic acid; peptides (200 μM) were added as indicated. The aliquots were incubated for 1 h at 4 or 37°C, centrifuged for 5 min at 16,000 *g* and neutralized when necessary. The lysates were incubated with 10 μg/ml of purified anti-rat/mouse I-A mAb OX6 (15) and the immune complexes were precipitated using Protein A–Sepharose precoated with rabbit anti-mouse IgG1 polyclonal antibodies (PharMingen, San Diego, CA). The precipitates were washed, resuspended in a sample buffer containing 2% SDS and 0.77 M 2-mercaptoethanol, and either boiled for 5 min or incubated for 40 min at room temperature. The eluted proteins were analyzed by SDS–PAGE in 10% gels. The gels were fixed, soaked in 1 M sodium salicylate (for ^{35}S-containing gels), dried and autoradiographed. Each lane represents 2×10^7 splenocytes.

Computer modeling

The structures of I-A^{g7} and of I-A^{g7}–peptide complexes were modeled by homology to the solved crystal structures of the human MHC class II molecule HLA-DR1 (16) and of the DR1–peptide complex (17). The models were built using the HOMOLOGY program (Biosym Technologies, San Diego, CA) and energy minimized using the ENCAD program (18).

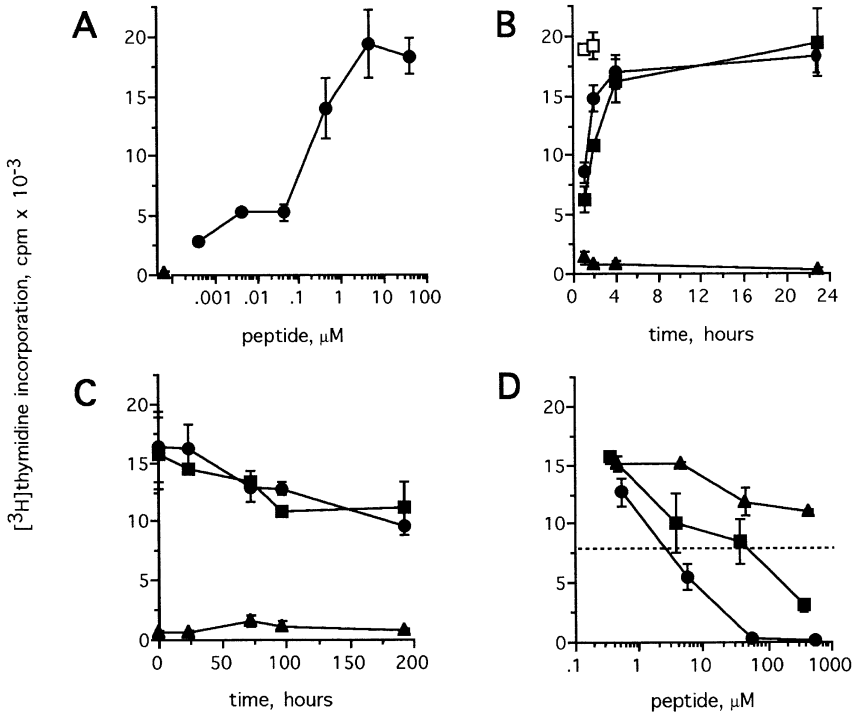

Fig. 1. The interaction of I-A^{g7} with peptides. The binding of peptide p12 to I-A^{g7} on the surface of glutaraldehyde-fixed macrophages was detected by the proliferation of a p12–I-A^{g7}-specific T cell line. The results represent mean ± SD thymidine incorporation (c.p.m.×10^{-3}) of duplicate cultures. (A) The dose-dependent binding of p12 to I-A^{g7}. Peptide binding was performed at pH 7.2 for 24 h. An inserted triangle shows the T cell response in the absence of the peptide. (B) The association of p12 with I-A^{g7}. The binding of 4 (squares) and 40 (circles) μM of p12 at pH 7.2, and of 4 μM (open squares) at pH 5.0 is shown. The triangles represent the response in the absence of the peptide. (C) The dissociation of p12 from I-A^{g7}. The cells were incubated with p12, washed and incubated at pH 7.2 for the indicated periods of time in buffer alone (circles) or in the presence (squares) of another I-A^{g7}-binding peptide, transferrin 336–349 (see D). The triangles represent the response in the absence of bound p12. (D) The competitive binding of peptides to I-A^{g7}. The fixed macrophages were incubated with 1 μM of p12 and with a dose range of test competing peptides for 2 h at pH 5.0. The competing peptides were mouse transferrin 336–349 (circles), mouse GAD 509–528 (squares) or rat ribophorin I 203–218 (triangles).

Results

The peptide binding capacity of I-A^{g7}

To examine the ability of I-A^{g7} to bind peptides, we used an assay based on peptide binding to MHC class II molecules on the surface of fixed macrophages (11). Effective binding of a peptide is detected by the proliferation of a peptide-specific CD4$^+$ T cell line. Although this assay does not allow precise biochemical analysis of the peptide–MHC interaction, the general characteristics of binding can be established. As a model peptide, we used peptide 166–185 of the mouse HSP60 protein, termed p12, which is strongly immunogenic in the NOD mice (J. Bočková *et al.*, in preparation). Peptide p12 binds I-A^{g7} in a dose-dependent, saturable manner (Fig. 1A). As illustrated in Fig. 1(B), p12 manifested slow association with I-A^{g7} ($t_{1/2}$ = 1.5 h) which was greatly enhanced at mildly acidic pH. Once formed, the p12–I-A^{g7} complex appeared very stable (Fig. 1C), as significant T cell activation was still observed after 8 days of dissociation (the $t_{1/2}$ was estimated to be 250 h using a single exponential fit). Moreover, similar experiments using unfixed splenic antigen-presenting cells revealed that p12 also persisted in living cells; >50% of the initial T cell response was still observed after 24 h of dissociation (data not shown). These parameters of peptide binding are similar to those observed with other MHC class II molecules (19).

To examine the specificity of peptide binding to I-A^{g7}, different peptides were tested for their ability to competitively inhibit the binding of p12. Figure 1(D) shows that a natural ligand of I-A^{g7}, mouse transferrin 336–349 (originally termed transferrin 55–68; ref. 7), and a previously described dominant T cell epitope, GAD 509–528 (20), were effective (ID_{50} = 3 and 40 μM respectively). In contrast, rat ribophorin I 203–218, a natural high-affinity ligand of the Lewis rat I-A molecule (11), showed poor binding (ID_{50} > 500 μM), confirming the specificity of the interaction.

The specificity of peptide binding to I-A^{g7}

To characterize the peptide binding specificity of I-A^{g7}, we designed a library of nonamer polyAla peptides with a set of amino acid substitutions at P1, P4, P6 and P9. Figure 2(A) illustrates the binding of the substituted polyAla peptides to I-A^{g7} measured in the competition binding assay. Peptide binding was done at pH 5.0. Figure 2 shows that I-A^{g7} has at least three anchor positions (P4, P6 and P9) with specific preferences for particular amino acid residues. At P4, the aliphatic Leu residue was favored; aromatic (Tyr) and small (Ala, Thr) residues were accepted, while large polar (Gln)

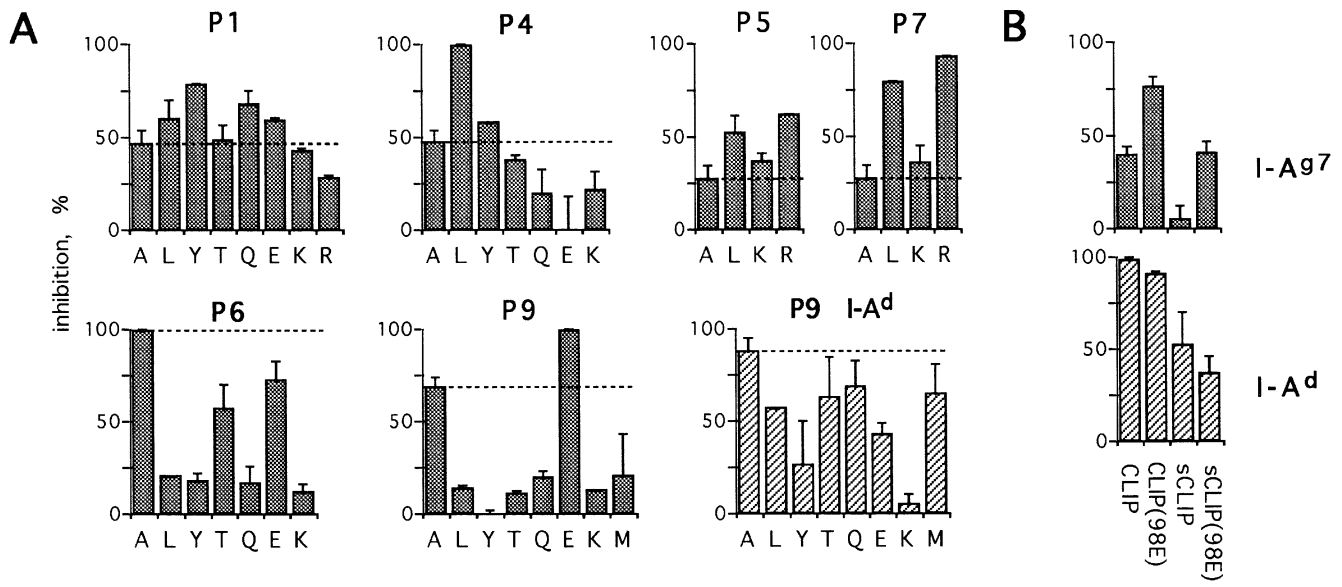

Fig. 2. The peptide binding specificity of I-A^{g7}. The binding of peptides to I-A^{g7} (dark bars) or to I-A^{d} (hatched bars) was measured in a competition binding assay (see Fig. 1D). Binding was measured at a single maximal concentration of the test peptide at pH 5.0. The data show percent inhibition ± SD of the response in the presence of control negatively binding peptides. (A) The binding of polyAla peptides substituted at the indicated positions. Dashed lines show the binding of an Ala-containing peptide. In the titration studies, 67 and 98% inhibition corresponded to ID_{50} of 200 and 10 μM respectively. (B) The binding of the invariant chain peptides 85–101 (CLIP) and 89–99 (sCLIP), and of their 98Met → Glu substitution variants.

and charged (Glu, Lys) residues decreased the binding. At P6, a strong preference for small residues (Ala, Thr) was observed; the apparent accommodation of Glu might result from a frameshift whereby the Glu residue actually served as anchor 9. At P9, the negatively charged Glu residue was favored while all other residues interfered with binding. Notably, P1 appeared to be degenerate, since all tested residues could be accommodated at this position. In addition, P1 was less important for binding than the other positions, since, in contrast to P4 and P9, no significant increase in binding was observed with any substitution at P1 (note that the same basic polyAla peptide was used for substitutions at P1 and P4).

Essentially the same results were obtained when the binding was performed at pH 7.2 (data not shown). However, the preference for Glu at P9 was less pronounced at neutral pH and other residues except Lys were accommodated, albeit less efficiently. This observation may explain the binding of peptides lacking an acidic residue at P9 (see below). At P6, moderate binding was observed with Leu, Asn and Glu, while Tyr, Gln and Lys abolished the binding completely.

In addition to the P4, P6 and P9 anchor positions, other positions could influence peptide binding to I-A^{g7} in a less specific manner. Indeed, as shown on Fig. 2(A), the introduction at P7 of Arg or Leu residues increased binding significantly. In contrast, only a moderate increase in binding was observed when these residues were placed at P5. The modeled structure of I-A^{g7} (see below) shows a large pocket at P7, which apparently can accommodate a broad variety of amino acids with a preference for large side chains.

Peptide binding to I-A^{g7} versus I-A^{d}

The preference for negatively charged residues at the C-terminal P9 anchor position appears to distinguish I-A^{g7} from other mouse I-A alleles. To study this point, we tested the set of peptides substituted at P9 for their binding to the highly homologous class II allele, I-A^{d}. Indeed, a different specificity of binding was observed in this case: the small Ala residue showed the best binding, while charged (Glu, Lys) and aromatic (Tyr) residues decreased binding significantly (Fig. 2A).

To confirm the correct assignment of the anchor positions in the experiments described above, we tested the binding of the mouse invariant chain 85–101 (CLIP) peptide to I-A^{g7} and I-A^{d}. The CLIP peptide contains a nonamer 'supermotif' sequence (amino acids 90–98: MRMATPLLM) which binds promiscuously to different MHC class II molecules by way of defined anchor positions (reviewed in 21). Figure 2(B) shows that CLIP bound moderately to I-A^{g7} (the binding was increased at neutral pH; data not shown) while the shorter 89–99 peptide (sCLIP) did not bind at all. However, the binding of both peptides was greatly enhanced by a 98Met → Glu substitution at P9. In contrast, this substitution did not enhance the binding of the CLIP peptides to I-A^{d}, consistent with a different specificity of P9 in I-A^{d}.

Molecular modeling of I-A^{g7}

The results observed above were consistent with a computer model of the I-A^{g7} structure and its interactions with peptides. The model was developed by homology to the solved crystal structure of HLA-DR1 (16) and of the DR1–peptide complex

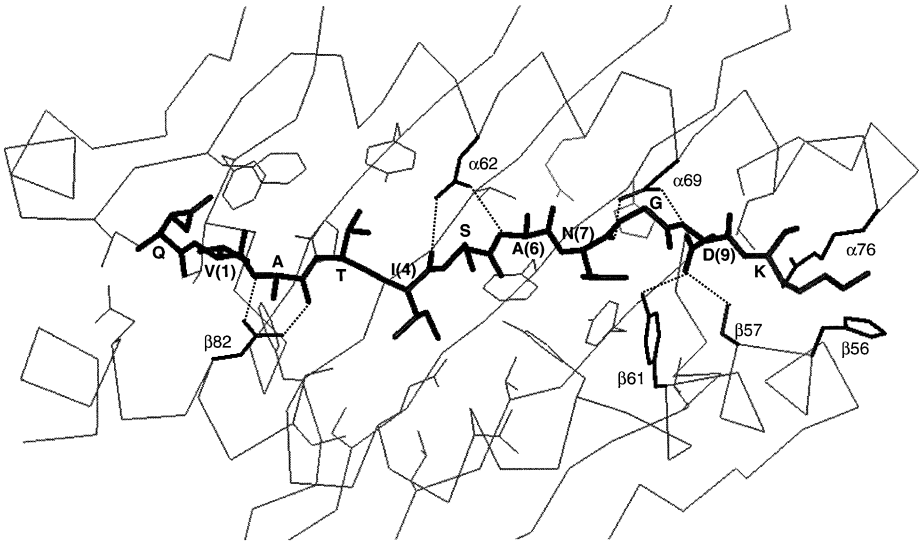

Fig. 3. Molecular modeling of I-A^{g7}. The computer model of the complex between I-A^{g7} and the core region of p12 (QVATISANGDK; J. Bočková *et al*., in preparation) is shown. The Asn residues in I-A^{g7} forming hydrogen bonds with the peptide backbone (α62, α69, β82) are highlighted. In addition, the rare β56His and β57Ser residues of I-A^{g7} and other residues important for the specificity of P9 (β61Tyr and α76Arg) are highlighted.

(17) (Fig. 3). The modeling showed a peptide binding groove similar to that of HLA-DR1, with prominent pockets at P1, P4, P6, P7 and P9. Since the critical Asn residues (α62, α69 and β82) involved in hydrogen bond formation with the peptide backbone are conserved in I-A^{g7}, the conformation of peptides in the binding groove would appear to be similar to that found in the HLA-DR1–peptide complex. Most importantly, it is the rare β57Ser residue of I-A^{g7} that apparently confers a preference for negatively charged residues at P9. The β57Ser residue both interacts directly with the P9 side chain and 'opens' the positive charge of α76Arg, which is otherwise involved in a salt bridge with β57Asp, at the bottom of the pocket. The other rare residue, β56His, in contrast, seems to project outside of the binding groove and is unlikely to influence the specificity of peptide binding.

The peptide binding motif of I-A^{g7}

The above results suggest that I-A^{g7} binds peptides by way of a typical MHC class II binding motif (10) containing at least three anchor positions P4, P6 and P9, as well as other less critical positions at P1 and P7. We sought the presence of this proposed motif in peptides known to interact with I-A^{g7}, including natural ligands, good binders and T cell epitopes of diabetes-related antigens in NOD mice. The binding of some of these peptides to I-A^{g7} was confirmed using the binding assay described above. Table 1 shows that the analyzed I-A^{g7}-binding peptides carry the proposed motif, confirming the specificity of peptide binding to I-A^{g7} *in vivo*. The alignment of some reported T cell epitopes (26,27) was more difficult, although the assignment of putative anchor positions was possible in each case (not shown). However, the actual affinity of these peptide epitopes for I-A^{g7} is not known and might, in fact, be quite low.

The trafficking and peptide occupancy of I-A^{g7} in cells

To analyze the intracellular behavior and *in vivo* peptide occupancy of I-A^{g7} proteins in comparison to other I-A alleles, we immunoprecipitated I-A molecules from splenocytes of different haplotypes. To facilitate the comparison, the I-A alleles were analyzed with a single mAb of broad specificity (15) that binds to I-A molecules at all stages of intracellular processing (28). Figure 4 shows the formation of SDS-resistant compact dimers (C), the form of class II molecules characteristic of stable peptide binding, by metabolically labeled mature I-A molecules. Note, at the top of the I-A^{s} NB lane, that I-A^{s} molecules form high mol. wt aggregates, which might represent a dimer of αβ heterodimers (29). As reported previously (9), a larger proportion (up to 75% as estimated by laser densitometry) of I-A^{g7} molecules was unstable in SDS, compared to the other I-A alleles (see α band). However, a significant fraction of SDS-resistant I-A^{g7} heterodimers (C) was consistently detected in these experiments.

Similar results were obtained when cell surface I-A molecules were analyzed. Figure 4(right panel) shows that, although the majority of surface I-A^{g7} were SDS-unstable, a fraction of compact I-A^{g7} dimers could be detected as well. These experiments also revealed the presence of low mol. wt material (arrow) which might represent class II-bound peptides labeled during cell surface iodination (30). Indeed, this material was not precipitated by an isotypic control mAb, had a mol. wt <3 kDa (data not shown) and did not appear when I-A heterodimers were not disrupted (see I-A^{s} NB lane). Note that this labeled material was present in the unboiled (NB) I-A^{g7} sample, suggesting that SDS-susceptible I-A^{g7} molecules might still contain bound peptides, as described previously for HLA-DR molecules (30).

To analyze the intracellular transport and to estimate the

Table 1. The alignment of peptides binding to I-A^{g7}

Protein	Epitope	Sequence	Binding	Reference.
		1 4 67 9		
(A) Naturally bound peptides				(7)
Transferrin	336–49	GNYVTA**I**R**N**QQ**E**G	+(3)	
MSA	560–74	kpKATAEQ**L**KT**V**M**D**d	yes	
hnRNP B1 and A2	31–43	ETTEES**L**R**N**YY**E**Q	yes	
hnRNP A2 and B1	51–66	VVMRD**P**A**S**KRSRGFGF	yes	
hnRNP A1	44–59	------**QT**--------	yes	
(B) Peptides binding to I-A^{g7}				
Z1a TCRβ	104–15	GHGTK**L**S**V**L**E**D**L**	+ (15)	[a]
M. t. HSP60	430–46	EGDEATGAN**I**V**K**V**A**L**E**A	+ (165)	[a]
Ovalbumin	323–39	ISQAVHA**A**H**A**E**I**NEAGR	yes	(22)[b]
λ repressor	12–26	LEDARR**L**K**A**I**Y**EKKK	yes	(22)
SNase	61–79	FTKKMVENAKK**I**E**V**EF**D**KG	yes	(22)
α1 antitrypsin	148–63	LSQAVHKA**V**L**T**I**D**ETG	yes	(22)
(C) Major T cell epitopes of diabetes-related antigens				
HSP60	437–60	vlgggvAL**L**RV**I**P**A**L**D**SLtpaned	+ (180)	(23[a])
HSP60	166–85	eeiaqVAT**I**S**A**N**G**D**K**eigni	+	[c]
GAD	524–43	srlSKVAPV**I**K**A**RMMeygtt	+	(20,24)
GAD	509–28	I**P**PS**L**R**T**L**E**D**N**EERMSRLSK	+ (40)	(20)
Insulin	B9–23	SHLVEALYL**V**C**G**ERG	+	(25)
CPH	362–82	KN**S**L**I**N**Y**L**E**QIHRGVKGFVK		(9)
CPH	440–64	FSPAVGVDFE**L**E**S**FS**E**RKEEEKEEL		(9)

Peptides known to interact with I-A^{g7} are aligned according to the proposed binding motif. Consensus residues at the major anchor positions are highlighted in bold; accepted residues at these positions as well as other preferred residues are underlined. Residues found to be dispensable for binding or for T cell responses are in lowercase. A '+' indicates that binding was confirmed in a competition binding assay (>90% inhibition at a single peptide concentration of 400–1000 μM). The ID_{50} (μM), if determined, is shown in parentheses. CPH, carboxypeptidase H; GAD, glutamic acid decarboxylase; *M. t.*, *Mycobacterium tuberculosis*, HSP60, heat-shock protein of 60 kDa mol.wt

[a]This study.

[b]The long peptides (HEL 13–35, myoglobin 131–153) as well as the non-immunogenic peptide (PSG-1 63–76), reported in this study to bind I-A^{g7}, could not be aligned unequivocally.

[c]J. Bočková *et al.*, in preparation.

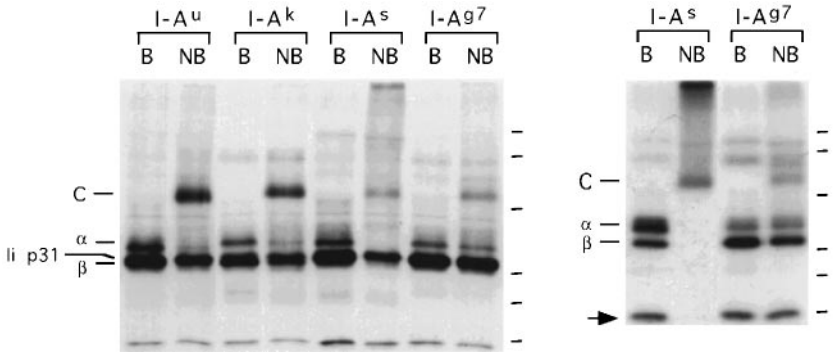

Fig. 4. Peptide occupancy of I-A^{g7} in cells. I-A molecules were immunoprecipitated from labeled splenocytes of the indicated haplotypes using mAb OX6. Each sample was dissolved in 2% SDS, divided into two aliquots and either boiled (B) or incubated at room temperature (NB) before SDS–PAGE. The bands corresponding to the invariant chain (Ii), the α and β chains and to the compact dimer (C) form of I-A are indicated. The positions of prestained SDS–PAGE standards (105, 82, 49, 33, 29 and 19 kDa) are marked. In the left panel, cells were pulsed with [^{35}S]methionine for 40 min, and chased for 4 h. On the right panel, cells were labeled with ^{125}I at the cell surface. The low mol. wt material possibly representing MHC-bound peptides (30) is indicated by an arrow.

lifespan of I-A^{g7} molecules in cells, a pulse–chase analysis of I-A^{g7} in comparison with I-A^{s} molecules was done (Fig. 5). It can be seen that newly synthesized I-A^{g7} and I-A^{s} molecules associated with the 31 and 41 kDa isoforms of the invariant chain (Ii). Subsequently, the amount of Ii decreased, consistent with its degradation in the endocytic compartment. Peptide binding, revealed by the presence of compact dimers (C), became apparent after 2 h of chase. Notably, I-A^{g7} molecules appeared to have as long a lifespan as did I-A^{s} (35–40% of α chains present after 2 h of chase were still

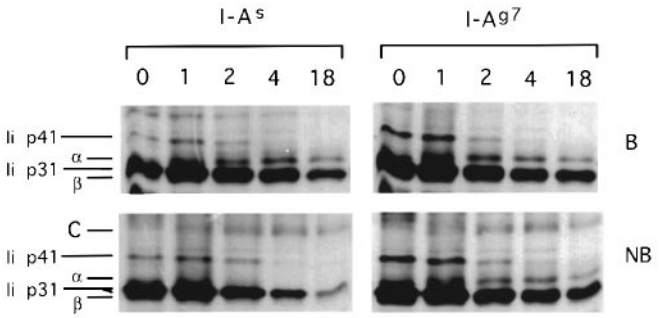

Fig. 5. Pulse–chase analysis of I-A^s and I-A^{g7} molecules. Splenocytes were pulsed with [^{35}S]methionine for 40 min. (0) and chased for 1, 2, 4 and 18 h. The I-A molecules were immunoprecipitated with OX6 and analyzed by SDS–PAGE with (B) or without (NB) boiling.

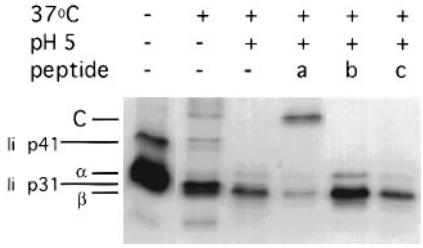

Fig. 6. Peptide binding to newly synthesized I-A^{g7} molecules. Splenocytes were pulsed for 30 min with [^{35}S]methionine and the lysates were treated for 1 h as indicated, before the immunoprecipitation of I-A molecules from the soluble fraction. The peptides used were p12 (a), Z1a TCRβ 104–15 (b) and ribophorin I 203–218 (c). The samples were not boiled before SDS–PAGE.

detected after 18 h, as determined by laser densitometry), and both SDS-stable (C) and unstable (α and β) forms of I-A^{g7} persisted in the cell for a comparably long time.

To directly assess the binding of peptides to I-A^{g7} molecules, we used the method developed by Germain and Rinker (14). In this system, the lysates of pulse-labeled cells are treated at acidic pH in the presence of peptides, which results in the dissociation of Ii and in peptide binding to newly synthesized empty class II molecules. We found that the dissociation of Ii is apparently caused by proteolysis rather than by acidic pH alone, since it was abrogated in the presence of protease inhibitors leupeptin and pepstatin (B. Reizis, unpublished). Figure 6 shows that the addition of peptide p12 induced the formation of the compact dimer form of I-A^{g7} (band C) confirming the ability of I-A^{g7} molecules to form stable SDS-resistant complexes with peptides. Other I-A^{g7}-binding peptides such as Z1a TCRβ 104–115 (Fig. 6) and transferrin 336–349 (data not shown) specifically increased the amount of precipitated I-A^{g7} molecules (see α and β bands) without the formation of compact dimers, as described previously for I-A^d molecules (14). These data show that I-A^{g7} molecules are capable of peptide binding without conversion to the compact dimer form. Furthermore, similar peptide treatments produced no effect on pulse–chased mature I-A^{g7} molecules (not shown), suggesting that at least some SDS-unstable mature I-A^{g7} heterodimers might be occupied with endogenous peptides (14).

Discussion

This study was undertaken to identify distinct molecular properties of the diabetes-associated mouse MHC class II molecule, I-A^{g7}. Here we report that I-A^{g7} binds peptides in the stable and specific manner typical of other MHC class II molecules. The binding of a model peptide to I-A^{g7} was stable both on fixed and on living cells, and was accompanied by the formation of SDS-resistant I-A^{g7} compact dimers. Some peptides were able to bind I-A^{g7} without inducing the formation of compact dimers, as reported for other MHC class II molecules (14,31). The I-A^{g7} molecule manifested a normal lifespan and a small, but clearly detectable fraction of I-A^{g7} formed compact dimers in the cell. Our results seem to contrast with those of Carrasco-Marin *et al.* (9) who reported that I-A^{g7} molecules are unable to bind peptides stably, have a reduced lifetime and only a negligible proportion (0–4%) appear as compact dimers in the cell. The discrepancy between our findings and those of Carrasco-Marin *et al.* could have arisen due to the different reagents and experimental systems used in the two studies. Be that as it may, our findings are consistent with the successful isolation of peptides naturally bound to I-A^{g7} (7). Moreover, stable peptide binding to I-A^{g7} would be expected in view of the fact that NOD mice are capable of mounting vigorous peptide-specific T cell responses and of positively selecting a diverse T cell repertoire. Thus, the association of I-A^{g7} with diabetes cannot be attributed to faulty peptide binding alone.

Similar to Carrasco-Marin *et al.* (9), we found that compared to several other I-A alleles, a relatively small fraction of I-A^{g7} appears as the SDS-resistant form in the cells. However, here we show that this instability of I-A^{g7}–peptide complexes cannot be accounted for by a general inability of I-A^{g7} to bind peptides. Moreover, the SDS-unstable I-A^{g7} molecules apparently maintained a normal lifespan, were associated with a low mol. wt material consistent with bound peptides and, unlike newly synthesized Ii-free molecules, could not be converted to compact dimers upon addition of peptides. Therefore, our data suggest that at least some of the SDS-unstable I-A^{g7} molecules might still contain bound peptides, as reported previously for other MHC class II molecules (14,30).

The molecular basis and functional consequences of the small amount of SDS-resistant I-A^{g7}–peptide complexes *in vivo* are not clear at present. Carrasco-Marin *et al.* (9) demonstrated that the small amount of the compact dimer form is not determined by the rare β57/β56 residues of I-A^{g7}. Similarly, we have found that the bulk of rat I-A molecule, RT1.B, is expressed in the compact dimer form despite the presence, as in I-A^{g7}, of Ser (RT1.B^{l,n}) or Asp (RT1.B^a) at position β57 (not shown). SDS-unstable class II–peptide complexes were reported to have a shorter intracellular lifespan than SDS-stable complexes (32); therefore, one can speculate that SDS-unstable peptide–I-A^{g7} complexes might affect T cell selection in the thymus or favor a particular type of T cell responses, perhaps a predominantly T_h1 responses. However, we found that SDS-unstable I-A^{g7} molecules persisted in the cells for a long time. In addition, the closely homologous I-A^d molecules are also mainly SDS-unstable (33), suggesting that this property is not unique to I-A^{g7} molecules.

It is possible, however, that a large fraction of I-A^{g7} molecules in cells is empty. Indeed, the yield of peptides isolated from purified I-A^{g7} molecules was found to be very low (H.-G. Rammensee, pers. commun.). Furthermore, the binding of peptide p12 to I-A^{g7} at the surface of fixed antigen-presenting cells occurred at much lower peptide concentrations than those required for other peptide–I-A combinations (not shown), a finding compatible with a larger fraction of empty I-A^{g7} at the cell surface. To explain this, one could suppose that empty I-A^{g7} heterodimers might be unusually stable in the absence of bound peptide. Indeed, it can be noted in Fig. 6 that the amount of I-A^{g7} heterodimer did not decrease upon the removal of Ii in the acidic environment; in contrast, other I-A molecules such as I-A^{k} and I-A^{s} were lost under these conditions (14 and our unpublished observations). In this regard, we noted a unique combination of residues (α66Glu/β9His) in the binding groove of I-A^{g7}, which could potentially form an intramolecular bond stabilizing the molecule in the absence of a peptide in the groove. In principle, these features of I-A^{g7} might be important for the presentation of autoantigenic peptides in the islets. Further studies using Ii- and peptide-free I-A^{g7} molecules are required to analyze the stability of empty I-A^{g7} heterodimers compared to other alleles and its possible relevance to diabetes in NOD mice.

Other workers have suggested peptide binding motifs for I-A^{g7} (7,27), but these motifs are not consistent with the general scheme of MHC class II binding motifs (10). Our present analysis is based on the assumption, supported by molecular modeling, that I-A^{g7} might manifest the same spacing of anchor positions as other class II alleles. Although a systematic exchange of every position in a peptide is still required to identify all amino acid preferences at each position, our approach has identified major anchor positions using an affordable number of synthesized peptides. Our data suggest a typical class II binding motif of nine residues with conserved anchor positions P4, P6 and P9. P1, in contrast, seems to be degenerate and not particularly important for binding. The degenerate nature of P1 is in good agreement with the recently characterized binding motifs of the RT1.B (11) and HLA-DQ (34,35) molecules, the rat and human homologs of mouse I-A. Other less conserved positions, such as P7, also seem to influence peptide binding to I-A^{g7} and require further analysis. Despite these reservations, we could detect the proposed binding motif in the known peptide ligands of I-A^{g7} as well as in diabetes-related T cell epitopes. Therefore, our data might be useful for the prediction and design of T cell epitopes for the experimental study of diabetes in NOD mice.

The importance of negatively charged residues near the C-terminus of I-A^{g7}-bound peptides was reported previously (7) and was correlated with either the β56His or β57Ser residues of I-A^{g7}. Similarly, here we demonstrate an allele-specific preference for negatively charged amino acids at anchor P9 in the I-A^{g7} motif. Our computer modeling suggests that the β57Ser residue of I-A^{g7} is primarily responsible for this specificity. Indeed, the same preference for negatively charged residues at P9 was observed by us for the Lewis rat I-A molecule, RT1.B^{l} (11), and by others for the HLA-DRB1*0405 molecule (8), both of which harbor the rare β57Ser residue.

Due to the rare, albeit not unique, specificity of P9, the overall peptide binding motif of I-A^{g7} should be quite different from the motifs of other mouse class II alleles which have an Asp residue at β57. Therefore, many peptides binding to I-A^{g7}, possibly including diabetogenic self-peptides, would not be presented by other mouse class II molecules. Indeed, the association of different HLA-DR alleles with rheumatoid arthritis was recently shown to correlate with their distinct binding specificities (10,36). Thus, it is likely that the peptide binding specificity of I-A^{g7} plays a major role in the association of I-A^{g7} with diabetes. Interestingly, the peptide binding motifs of I-A^{g7} and of the diabetes-associated human MHC class II molecule HLA-DQA1*0301/B1*0302 (35) appear quite similar, possibly allowing many of the same peptides to be presented by both molecules. Thus, it is possible that diabetes in mice and humans might have a similar immunopathogenesis and even might involve the same autoantigenic peptides.

Acknowledgements

We thank Aviva Kapitkovsky for peptide synthesis and Dr Hans-Georg Rammensee for communicating unpublished data. The study was supported in part by the Ministry of Science of Israel and the Council for Science and Technology of Japan. I. R. C. is the incumbent of the Mauerberger Chair in Immunology and the Director of the Robert Koch-Minerva Center for Research in Autoimmune Diseases. M. E. was supported by the Kimmelman Center for Macromolecular Assembly.

Abbreviations

NOD non-obese diabetic

References

1 Kikutani, H. and Makino, S. 1992. The murine autoimmune diabetes model: NOD and related strains. *Adv. Immunol.* 51:285.
2 Bach, J. F. 1995. Insulin-dependent diabetes mellitus as a β-cell targeted disease of immunoregulation. *J. Autoimmun.* 8:439.
3 Wicker, L. S., Todd, J. A. and Peterson, L. B. 1995. Genetic control of autoimmune diabetes in the NOD mouse. *Annu. Rev. Immunol.* 13:179.
4 Acha-Orbea, H. and McDevitt, H. O. 1987. The first external domain of the nonobese diabetic mouse class II I-A β chain is unique. *Proc. Natl Acad. Sci. USA* 84:2435.
5 Steinman, L. 1995. Escape from 'Horror Autotoxicus': pathogenesis and treatment of autoimmune disease. *Cell* 80:7.
6 Thorsby, E. 1995. HLA-associated disease susceptibility—which genes are primarily involved? *The Immunologist* 3:51.
7 Reich, E.-P., von Grafenstein, H., Barlow, A., Swenson, K. E., Williams, K. and Janeway, C. A., Jr. 1994. Self peptides isolated from MHC glycoproteins of non-obese diabetic mice. *J. Immunol.* 152:2279.
8 Rammensee, H.-G., Friede, T. and Stefanoviç, S. 1995. MHC ligands and peptide motifs: first listing. *Immunogenetics* 41:178.
9 Carrasco-Marin, E., Shimizu, J., Kanagawa, O. and Unanue, E. R. 1996. The class II MHC I-A^{g7} molecules from non-obese diabetic mice are poor peptide binders. *J. Immunol.* 156:450.
10 Rammensee, H.-G. 1995. Chemistry of peptides associated with MHC class I and class II molecules. *Curr. Opin. Immunol.* 7:85.
11 Reizis, B., Mor, F., Eisenstein, M., Schild, H., Stefanoviç, S., Rammensee, H.-G. and Cohen, I. R. 1996. The peptide binding specificity of the MHC class II I-A molecule of the Lewis rat, RT1.B^{l}. *Int. Immunol.*, in press.
12 Buus, S., Sette, A., Colon, S. M., Miles, C. and Grey, H. M. 1987. The relation between major histocompatibility complex (MHC) restriction and the capacity of Ia to bind immunogenic peptides. *Science* 235:1353.

13 Könen-Waisman, S., Fridkin, M. and Cohen, I. R. 1995. Self and foreign 60-kilodalton heat shock protein T cell epitope peptides serve as immunogenic carriers for a T cell-independent sugar antigen. *J. Immunol.* 154:5977.
14 Germain, R. N. and Rinker, A. G., Jr. 1993. Peptide binding inhibits protein aggregation of invariant chain-free class II dimers and promotes surface expression of occupied molecules. *Nature* 363:725.
15 McMaster, W. R. and Williams, A. F. 1979. Identification of Ia glycoproteins in rat thymus and purification from rat spleen. *Eur. J. Immunol.* 9:426.
16 Brown, J. H., Jardetzky, T. S., Gorga, J. C., Stern, L. J., Urban, R. G., Strominger, J. L. and Wiley, D. C. 1993. Three-dimensional structure of the human class II histocompatibility antigen HLA-DR1. *Nature* 364:33.
17 Stern, L. J., Brown, J. H., Jardetzky, T. S., Gorga, J. C., Urban, R. G., Strominger, J. L. and Wiley, D. C. 1994. Crystal structure of the human class II MHC protein HLA-DR1 complexed with an influenza virus peptide. *Nature* 368:215.
18 Levitt, M. 1983. Molecular dynamics of native protein I. Computer simulation of trajectories. *J. Mol. Biol.* 168:595.
19 Germain, R. N. and Margulies, D. H. 1993. The biochemistry and cell biology of antigen processing and presentation. *Annu. Rev. Immunol.* 11:403.
20 Kaufmann, D. L., Clare-Salzler, M., Tian, J., Forsthuber, T., Ting, G. S. P., Robinson, P., Atkinson, M. A., Sercarz, E. E., Tobin, A. J. and Lehmann, P. V. 1993. Spontaneous loss of T-cell tolerance to glutamic acid decarboxylase in murine insulin-dependent diabetes. *Nature* 366:69.
21 Busch, R. and Mellins, E. 1996. Developing and shedding inhibitions: how MHC class II molecules reach maturity. *Curr. Opin. Immunol.* 8:51.
22 Vaysburd, M., Lock, C. and McDevitt, H. O. 1995. Prevention of insulin-dependent diabetes mellitus in nonobese diabetic mice by immunogenic but not by tolerated peptides. *J. Exp. Med.* 182:897.
23 Elias, D., Reshef, T., Birk, O. S., van der Zee, R., Walker, M. D. and Cohen, I. R. 1991. Vaccination against autoimmune mouse diabetes with a T-cell epitope of the human 65 kDa heat shock protein. *Proc. Natl Acad. Sci. USA* 88:3088.
24 Quinn, A. and Sercarz, E. 1995. Analysis and modulation of the anti-GAD response in the NOD mouse. In: *Immunology of Diabetes '95.* Abstracts. *Autoimmunity* 21:25.
25 Daniel, D., Gill, R. G., Schloot, N. and Wegmann, D. 1995. Epitope specificity, cytokine production profile and diabetogenic activity of insulin-specific T cell clones isolated from NOD mice. *Eur. J. Immunol.* 25:1056.
26 Deng, H., Apple, R., Clare-Salzler, M., Trembleau, S., Mathis, D., Adorini, L. and Sercarz, E. 1993. Determinant capture as a possible mechanism of protection afforded by major histocompatibility complex class II molecules in autoimmune diseases. *J. Exp. Med.* 178:1675.
27 Amor, S., O'Neill, J. K., Morris, M. M., Smith, R. M., Wraith, D. C., Groome, N., Travers, P. J. and Baker, D. 1996. Encephalitogenic epitopes of myelin basic protein, proteolipid protein and myelin oligodendrocyte glycoprotein for experimental allergic encephalomyelitis induction in Biozzi ABH (H-2A^{g7}) mice share an amino acid motif. *J. Immunol.* 156:3000.
28 Reske, K. and Weitzel, R. 1985. Immunologically discrete conformation isomers of I-A locus-equivalent class II molecules detected in Lewis rats. *Eur. J. Immunol.* 15:1229.
29 Schafer, P. H. and Pierce, S. K. 1994. Evidence for dimers of MHC class II molecules in B lymphocytes and their role in low affinity T cell responses. *Immunity* 1:699.
30 Lanzavecchia, A., Reid, P. A. and Watts, C. 1992. Irreversible association of peptides with class II MHC molecules in living cells. *Nature* 357:249.
31 Nelson, C. A., Petzold, S. J. and Unanue, E. R. 1993. Identification of two distinct properties of class II major histocompatibility complex-associated peptides. *Proc. Natl Acad. Sci. USA* 90:1227.
32 Nelson, C. A., Petzold, S. J. and Unanue, E. R. 1994. Peptides determine the lifespan of MHC class II molecules in the antigen-presenting cell. *Nature* 371:250.
33 Germain, R. N. and Hendrix, L. R. 1991. MHC class II structure, occupancy and surface expression determined by post-endoplasmic reticulum antigen binding. *Nature* 353:134.
34 Johansen, B. H., Vartdal, F., Eriksen, J. A., Thorsby, E. and Sollid, L. M. 1996. Identification of a putative motif for binding of peptides to HLA-DQ2. *Int. Immunol.* 8:177.
35 Kwok, W. W., Domeier, M. E., Raymond, F. C., Byers, P. and Nepom, G. T. 1996. Allele-specific motifs characterize HLA-DQ interactions with a diabetes-associated peptide derived from glutamic acid decarboxylase. *J. Immunol.* 156:2171.
36 Hammer, J., Gallazzi, F., Bono, E., Karr, R. W., Guenot, J., Valsasnini, P., Nagy, Z. A. and Sinigaglia, F. 1995. Peptide binding specificity of HLA-DR4 molecules: correlation with rheumatoid arthritis. *J. Exp. Med.* 181:1847.